

目次

基于时间序列分解的京津冀区域PM_{2.5}和O₃空间分布特征姚青,丁净,杨旭,蔡子颖,韩素芹 (2487)

基于随机森林的北京城区臭氧敏感性分析周红,王鸣,柴文轩,赵昕 (2497)

基于随机森林模型的四川盆地臭氧污染预测杨晓彤,康平,王安怡,臧增亮,刘浪 (2507)

海口市臭氧浓度统计预报模型的构建与效果评估符传博,林建兴,唐家翔,丹利 (2516)

京津冀地区2015~2020年臭氧浓度时空分布特征及其健康效益评估高冉,李琴,车飞,张艳平,祖永刚,刘芬 (2525)

2022年北京市城区PM_{2.5}水溶性离子含量及其变化特征陈圆圆,崔迪,赵泽熙,常森,景宽,沈秀娥,刘保献 (2537)

郑州市冬春季PM_{2.5}中金属元素污染特征、来源及健康风险评估陶杰,闫慧姣,徐艺斐,荆海涛 (2548)

淄博市供暖前后PM_{2.5}中多环芳烃及其衍生物污染特征、来源及健康风险孙港立,吴丽萍,徐勃,高玉宗,赵雪艳,姬亚芹,杨文 (2558)

西安市采暖季过渡期高时间分辨率细颗粒物组分特征及来源解析李萌津,张勇,张倩,田杰,李丽,刘卉昆,冉伟康,王启元 (2571)

天津冬季两个典型污染过程高浓度无机气溶胶成因及来源分析卢苗苗,韩素芹,刘可欣,唐晓,孔磊,丁净,樊文雁,王自发 (2581)

基于空间尺度效应的山东省PM_{2.5}浓度时空变化及空间分异地理探测徐勇,韦梦新,邹滨,郭振东,李沈鑫 (2596)

我国典型化工行业VOCs排放特征及其对臭氧生成潜势武婷,崔焱文,肖成德,翟增秀,韩萌 (2613)

廊坊秋季大气污染过程中VOCs二次气溶胶生成潜势及来源分析张敬巧,刘铮,丁文文,朱瑶,曹婷,凌德印,王淑兰,王宏亮 (2622)

景观格局对河流水质影响的尺度效应Meta分析王玉仓,杜晶晶,张禹,吴昊,胡敏韵,陈丁江 (2631)

白洋淀夏季汛期入淀河流水体溶解性有机物的光谱特征及来源孟佳靖,婁红,陈哲,周石磊,底怡玲,武辰彬,王晨光,张家丰,崔建升 (2640)

北京市丰台区永定河以东浅层地下水水化学演变规律及成因分析胡昱欣,周瑞静,宋炜,杨全合,王鑫茹 (2651)

庐庐断裂带(安徽段)浅层地下水水化学特征、控制因素及水质评价刘海,魏伟,宋阳,徐洁,管政亭,黄健敏,赵国红 (2665)

农药施用对兴凯湖水中农药残留的影响及其风险评价王蔚青,徐雄,刘权震,林利华,吕婧,王东红 (2678)

黄河兰州段河岸带土壤中微生物与耐药基因的赋存特征韦程宸,魏枫沂,夏慧,黄魁 (2686)

基于多源数据的巢湖蓝藻水华时空分布及驱动因素分析金晓龙,邓学良,戴睿,徐倩倩,吴月,范裕祥 (2694)

再生水构建水环境中沉水植物附着细菌群落特征贺赞,李雪梅,李宏权,魏琳琳,姜春晖,姜大伟,李魁晚 (2707)

水位波动和植被恢复对三峡水库消落带土壤原核微生物群落结构的交互影响梅渝,黄平,王鹏,朱凯 (2715)

银川市典型湖泊沉积物细菌群落结构及其对重金属的响应关系蒙俊杰,刘双羽,邱小琼,周瑞娟 (2727)

热水解时间对污泥厌氧消化系统微生物群落结构影响分析张含,张涵,王佳伟,高金华,文洋,李相昆,任征然 (2741)

市政污水中吗啡来源辨析邵雪婷,赵悦彤,蒋冰,裴伟,李彦莹,谭冬芹,王德高 (2748)

溱沔河流域生态环境动态遥感评价李艳翠,袁金国,刘博涵,郭豪 (2757)

黄河流域生态系统服务价值时空演化及影响因素王奕洪,洪学莹 (2767)

基于贝叶斯网络的生态系统服务权衡协同关系强度及其空间格局优化:以汾河流域为例蔡进,危小建,江平,梁玉琦 (2780)

贵州高原典型喀斯特县域生境质量时空演变及定量归因李月,冯霞,吴路华,罗光杰,罗红芬 (2793)

2000~2021年黄土高原生态分区NEP时空变化及其驱动因子周怡婷,严俊霞,刘菊,王璞 (2806)

基于SSP-RCP情景的黄土高原土地变化模拟及草原碳储量崔霞,董燕,张露尹,王荣耀 (2817)

京津冀城市群建设用地扩张多情景模拟及其对生态系统碳储量的影响武爱彬,陈辅国,赵艳霞,秦彦杰,刘欣,郭小平 (2828)

西南岩溶区土地利用变化对团聚体稳定性及其有机碳的影响江可,贾亚男,杨琰,陈坚淇,禹朴家 (2840)

不同土地利用方式下土壤有机质分子组成变化的整合分析黄世威,赵一锴,朱馨雨,刘贺雷,刘姣姣,陈稍,陈佳永,张阿凤 (2848)

基于改进麻雀搜索算法优化BP神经网络的土壤有机质空间分布预测胡志瑞,赵万伏,宋根先,王芳,林妍敏 (2859)

不同有机物料施用对菜地磷累积和转化的影响孙凯,崔玉涛,李顺晋,魏冰丽,王媛,杨宏博,王孝忠,张伟 (2871)

集约化柑橘种植抑制土壤磷循环微生物活性周连昊,曾全超,梅唐英泽,汪明霞,谭文峰 (2881)

控释掺混肥对麦玉米轮作体系作物产量和温室气体排放的影响高玮,王学霞,谢建治,陈延华,倪小会,王甲辰,董艳芳,李子双,曹兵 (2891)

生物炭对黄绵土中NO₃-N运移过程影响及模拟白一茹,刘旭,张钰涵,张睿媛,马艳,王幼奇 (2905)

中国农田土壤重金属污染分析与评价杨雳,白宗旭,薄文浩,林静,杨佩佳,陈涛 (2913)

城市土壤和地表灰尘重金属污染研究进展与展望王晓雨,刘恩峰,杨祥梦,王碧莲,林锦阔,颜梦霞,毕世杰 (2926)

场地重金属污染土壤固化及MICP技术研究进展陈玥如,高文艳,陈虹任,薛生国,吴川 (2939)

黄河流域山东段近河道煤矿区土壤重金属污染特征及源解析戴文婷,张晖,吴霞,钟鸣,段桂兰,董霖红,张培培,樊洪明 (2952)

拒马河流域河流沉积物与土壤重金属含量及风险评价韩双宝,袁磊,张秋霞,郑焰,李甫成 (2962)

银川市黄河滩区土壤重金属污染特征、生态风险评估及来源解析于路加,马海军,王翠平 (2971)

基于源导向和蒙特卡罗模型的广东省某城市土壤重金属健康风险评估陈莲,邹子航,张培珍,王雨菡,王振江,林森,唐翠明,罗国庆,钟建武,李智毅,王圆 (2983)

西南典型碳酸盐岩高地背景区农田重金属化学形态、影响因素及回归模型唐瑞玲,徐进力,刘彬,杜雪苗,顾雪,于林松,毕婧 (2995)

贵州省水田土壤-水稻Hg含量特征与安全种植区划韦美溜,周浪,黄燕玲,庞瑞,王佛鹏,宋波 (3005)

柠檬酸辅助甜高粱对南方典型母质土壤的镉修复效应刘梦宇,罗绪锋,辜娇峰,易轩韬,周航,曾鹏,廖柏寒 (3016)

改性酒糟生物炭对紫色土壤镉形态及水稻吸收镉的影响肖乃川,王子芳,杨文娜,谢永红,代文才,高明 (3027)

生物炭对四环素和铜复合污染土壤生菜生长及污染物累积的影响郑晨格,裴欢欢,张亚珊,李嘉欣,刘奋武,乔星星,秦俊梅 (3037)

基于Meta分析的蚯蚓堆肥对堆肥质量和重金属的影响效应姜继韶,侯睿,崔慧林,闫广轩,刘栋 (3047)

微塑料对土壤N₂O排放及氮素转化的影响研究进展刘一戈,杨安琪,陈舒欣,牛奕奕,卢瑛,李博 (3059)

土地利用对洱海罗时江小流域土壤微塑料污染的影响戴柳云,侯磊,王化,符立松,王艳霞,李晓琳,王万宾,梁启斌 (3069)

养殖海湾淤泥质海岸沉积物微塑料污染特征宋可心,贺金成,李昌文,解思琦,刘宝莹,黄伟,冯志华 (3078)

聚乙烯微塑料对盐渍化土壤微生物群落的影响王志超,李哲,李嘉辰,屈忠义,胡文煊,李卫平 (3088)

鄱阳湖候鸟栖息地微塑料表面细菌群落结构特征与生态风险预测俞锦丽,赵俊凯,罗思琦,景文慧,杨启武,刘淑丽 (3098)

粤闽浙沿海重点城市道路交通节能减排路径徐艺诺,翁大维,王硕,胡喜生,王占永,张园园,张兰怡 (3107)

电动重卡替代柴油重卡的全生命周期碳减排效益分析徐圆圆,龚德鸿,黄正光,杨浪 (3119)

基于随机森林的北京城区臭氧敏感性分析

周红¹, 王鸣^{1*}, 柴文轩², 赵昕³

(1. 南京信息工程大学环境科学与工程学院, 江苏省大气环境与装备技术协同创新中心, 江苏省大气环境监测与污染控制高新技术研究重点实验室, 南京 210044; 2. 中国环境监测总站, 北京 100012; 3. 南京科略环境科技有限责任公司, 南京 211800)

摘要: 明确臭氧(O₃)与前体物的非线性关系是O₃防控措施制定的基础和关键。基于北京城区站点2020年4~9月O₃、挥发性有机物(VOCs)、氮氧化物(NO_x)和气象要素在线观测, 分析了O₃及其前体物污染特征, 利用随机森林(RF)模型结合SHAP值探究了影响O₃的关键因素, 并通过多情景分析探讨了O₃-VOCs-NO_x敏感性。相关性分析结果显示O₃小时浓度与温度(*T*)呈显著正相关, 与TVOCs和NO_x呈显著负相关; 但从每日结果来看, O₃与*T*、TVOCs和NO_x均呈显著正相关。RF模型模拟的O₃浓度与实测值吻合较好, 进一步计算了各个特征变量的SHAP值, 结果显示*T*和NO_x对O₃影响最高, 但前者是正向影响, 而后者是负向影响。以观测期间O₃污染天的NO_x和VOCs平均值为基础情景, 设置了对应不同NO_x和VOCs的多种情景, 并利用RF模型计算不同情景下的O₃, 得到O₃等值线(EKMA曲线), 结果显示北京城区O₃-VOCs-NO_x敏感性处于VOCs控制区, 与基于观测的盒子模型(OBM)得到的结果一致, 这说明RF模型可以用作O₃-VOCs-NO_x敏感性分析的一种补充方法。

关键词: 北京; 臭氧(O₃); O₃-VOCs-NO_x敏感性; 随机森林(RF); SHAP值

中图分类号: X515 文献标识码: A 文章编号: 0250-3301(2024)05-2497-10 DOI: 10.13227/j.hjxx.202306034

Ozone Sensitivity Analysis in Urban Beijing Based on Random Forest

ZHOU Hong¹, WANG Ming^{1*}, CHAI Wen-xuan², ZHAO Xin³

(1. Collaborative Innovation Center of Atmospheric Environment and Equipment Technology, Jiangsu Key Laboratory of Atmospheric Environment Monitoring and Pollution Control, School of Environmental Science and Engineering, Nanjing University of Information Science & Technology, Nanjing 210044, China; 2. China National Environmental Monitoring Centre, Beijing 100012, China; 3. Nanjing Intelligent Environmental Science and Technology Co., Ltd., Nanjing 211800, China)

Abstract: The basis and key step to developing ozone (O₃) prevention and control measures is determining the non-linear relationship between O₃ and its precursors. Based on online observations of O₃, volatile organic compounds (VOCs), nitrogen oxides (NO_x), and meteorological elements from April to September 2020 at an urban site in Beijing, we analyzed the pollution characteristics of O₃ and its precursors, explored key factors affecting O₃ using the random forest (RF) model combined with SHAP values, and explored the O₃-VOCs-NO_x sensitivity through a multi-scenarios analysis. The results of correlation analysis showed that the hourly concentration of O₃ was significantly positively correlated with temperature (*T*) and negatively correlated with TVOCs and NO_x. However, in terms of the daily values, O₃ was significantly positively correlated with *T*, TVOCs, and NO_x. The simulated O₃ values by the RF model agreed with the measured values. The SHAP values of each characteristic variable were further calculated. The results suggested that *T* and NO_x showed the two highest effects on O₃, with positive and negative values, respectively. Based on the average NO_x and VOCs on O₃ pollution days during the observation period (the base scenario), multi-scenarios with different NO_x and VOCs were set up. The RF model was used to calculate O₃ under different scenarios and obtain the O₃ isopleth (EKMA curve). The results showed that the O₃-VOCs-NO_x sensitivity in urban areas of Beijing was in the VOCs-limited regime, which was consistent with the results obtained from the observation-based box model(OBM). This indicated that the RF model could be used as a complementary method for O₃-VOCs-NO_x sensitivity analysis.

Key words: Beijing; ozone(O₃); O₃-VOCs-NO_x sensitivity; random forest (RF); SHAP value

近地面高浓度臭氧(O₃)会对人体健康和生态环境产生不利影响^[1-3], 同时也会导致温室效应的产生^[4]。2020年全国以O₃为首要污染物的超标天数占总超标天数的比例高达37.1%, 仅次于PM_{2.5}^[5]。其中, 京津冀地区以O₃为首要污染物的超标天数占总超标天数的46.6%, 与PM_{2.5}相当(48.0%)^[5], O₃污染已成为京津冀地区主要空气污染问题之一。近地面O₃主要由挥发性有机物(volatile organic compounds, VOCs)与氮氧化物(nitrogen oxides, NO_x = NO+NO₂)等前体物在光照下发生光化学反应生成^[6], 而且O₃生成与VOCs和NO_x呈高度非线性关系^[7,8]。因此, 开展O₃生成与前体物VOCs和NO_x(O₃-VOCs-NO_x)敏感性分析, 识别VOCs和NO_x在O₃生成中的作用, 是O₃

防控对策制定的基础和关键。

目前用于O₃-VOCs-NO_x敏感性分析的技术有: 基于排放的三维空气质量模型(emission-based model, EBMM)^[9,10]、基于观测的盒子模型(observation-based model, OBM)^[11-13]和机器学习(machine learning, ML)^[14,15]等。EBM需要输入详细的排放清单和气象场^[16], 而O₃前体物(尤其是VOCs)排放清单的不确定性可能影响O₃-VOCs-NO_x敏感性分析结果^[17,18]。OBM不需要输入排放清单^[19], 但会受到

收稿日期: 2023-06-05; 修订日期: 2023-08-04

基金项目: 国家自然科学基金项目(41505113)

作者简介: 周红(1998~), 女, 硕士研究生, 主要研究方向为基于机器学习的臭氧生成敏感性分析, E-mail: 20211248165@nuist.edu.cn

* 通信作者, E-mail: wangming@nuist.edu.cn

观测数据时空代表性的限制^[20]. ML运行速度快, 计算效率高^[21], 尤其适用于多站点长期数据的分析^[22,23]. 近年来, 利用ML来识别O₃前体物、气象要素等变量对O₃影响的研究逐步发展起来. 有研究基于随机森林(random forest, RF)^[24,25]、多元线性回归(multiple linear regression, MLR)^[25,26]和深度卷积神经网络(convolutional neural network, CNN)^[27]等ML方法对大气O₃浓度进行模拟, 并呈现出良好性能. Shapley加法解释算法(Shapley additive explanations, SHAP)是近年来常用的一种探究O₃生成关键驱动因素的方法. Wang等^[14]利用SHAP算法对兰州地区O₃生成敏感性进行分析, 发现减少VOCs可以降低O₃浓度, 但是减少NO_x反而导致O₃浓度增加, 这意味着O₃生成处于VOCs控制区. 另外, 目前基于ML的O₃研究大多采用实测的VOCs总量或组分数据^[28], 较少考虑VOCs在大气中的光化学消耗这一过程. Zhan等^[29]校正光化学消耗的影响, 计算VOCs初始体积分数, 利用RF模型探讨了2014~2016年夏季北京城区O₃生成的主要影响因素和O₃-VOCs-NO_x敏感性, 并与OBM模型进行比较, 发现ML与OBM所

得结果接近, 均认为O₃生成处于VOCs控制区.

本研究基于北京城区站点2020年4月1日至9月30日O₃、VOCs、NO_x、一氧化碳(CO)、风速(WS)、风向(WD)、相对湿度(RH)和温度(*T*)在线监测数据, 分析了O₃及其前体物VOCs和NO_x污染特征, 以及O₃与前体物和气象要素的相关性. 利用RF对O₃浓度进行模拟并评估其模拟效果, 并使用SHAP算法解释了每个特征变量对O₃浓度的贡献. 利用RF通过多情景分析探讨O₃-VOCs-NO_x敏感性, 与OBM结果进行比较和验证, 旨在为O₃-VOCs-NO_x敏感性分析提供一种更为快速简洁的方法.

1 材料与方法

1.1 外场观测

本研究中O₃及其前体物浓度和气象要素监测站点(BJ)位于北京市城区北部(116.42°E, 40.05°N, 图1), 距离北京市中心约16 km, 周边主要为住宅区, 无明显的局地排放源, 代表城市大气环境. 观测时间为2020年4~9月, 这一时间段光照强、温度高, 有利于O₃生成.

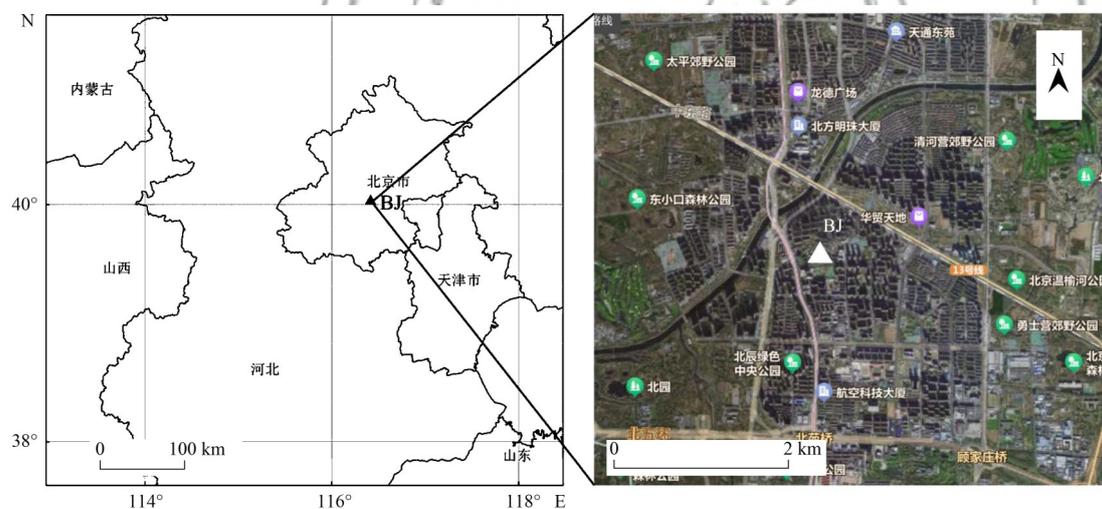


图1 观测站点(BJ)位置

Fig. 1 Location of the observation site (BJ)

本研究中大气VOCs利用无制冷剂自动气相色谱系统(GC-FID/MS, Agilent 5975/7890, 美国)进行在线监测. 该系统由超低温制冷装置、VOCs采样和预浓缩系统、气相色谱系统(GC)组成. 环境空气通过采样管路进入包含双气路的预浓缩系统, 在超低温条件下(-110°C)富集VOCs, 加热解析后进入GC, 分别利用PLOT和DB-624色谱柱进行分离, 然后利用氢火焰离子化检测器(FID)和质谱检测器(MS)进行定量检测^[30]. 观测VOCs物种包含57种非甲烷碳氢(29种烷烃、10种烯烃、1种炔烃和17种芳香烃), 时间分辨率为1 h. 所采用标气为商品化混合标气(1×10^{-6} ,

CNEMC Mix, Linde SPECTRA Environmental Gases, 美国), 将其稀释为体积分数为 $0.5 \times 10^{-9} \sim 8 \times 10^{-9}$ 的标气以便建立标准曲线. 各VOC组分标准曲线的可决系数 R^2 均高于0.99. 将低浓度标气重复测量7次, 计算出各VOC组分的方法检出限为 $0.003 \times 10^{-9} \sim 0.01 \times 10^{-9}$.

O₃、NO_x和CO分别使用紫外光度O₃分析仪(49i, Thermo Scientific, 美国)、化学发光NO-NO₂-NO_x分析仪(42i, Thermo Scientific, 美国)和红外吸收光谱仪(48i, Thermo Scientific, 美国)进行测量; 气象要素WD、WS、RH和*T*数据则由自动气象站(WXT520, Vaisala, 芬兰)测量.

1.2 光化学初始体积分数的计算

VOCs 测量体积分数反映了排放、物理和化学过程的综合影响^[31,32]. 假设 VOCs 排放进入大气后先混合均匀, 再经历光化学消耗(与 $\cdot\text{OH}$ 的氧化反应), 则可以计算 VOCs 光化学初始体积分数^[33]:

$$[\text{VOC}_j]_0 = \frac{[\text{VOC}_j]_t}{e^{-k_j \times [\cdot\text{OH}] \times \Delta t}} \quad (1)$$

式中, $[\text{VOC}_j]_t$ 和 $[\text{VOC}_j]_0$ 分别为观测到的 VOCs 组分 j 体积分数和未经历光化学反应时的初始体积分数. k_j 为 VOC 组分 j 与 $\cdot\text{OH}$ 的反应速率常数 [$\text{cm}^3 \cdot (\text{molecule} \cdot \text{s})^{-1}$], 数值来自文献^[34]. $[\cdot\text{OH}]$ 为 $\cdot\text{OH}$ 浓度平均值 ($\text{molecule} \cdot \text{cm}^{-3}$), Δt 为光化学反应时间 (s). 在计算时将 $([\cdot\text{OH}] \times \Delta t)$ 作为一个整体, 其通过两种 VOC 组分的比值计算得到, 公式如下:

$$[\cdot\text{OH}] \times \Delta t = \frac{1}{k_X - k_E} \times \left[\ln \left(\frac{X}{E} \right)_0 - \ln \left(\frac{X}{E} \right)_t \right] \quad (2)$$

式中, X 和 E 分别为间/对-二甲苯和乙苯. 选择二者的原因是其相关性强 ($r = 0.93$, $P < 0.05$), 表明其来源相近, 而且其化学活性有显著的差异. $(X/E)_t$ 为测量到的 X 和 E 体积分数比值. $(X/E)_0$ 为 X 和 E 未经历光化学反应时的初始体积分数比值, 通常根据光化学反应很弱时段(如夜间和清晨) $(X/E)_t$ 计算得到. 有研究分别选择了夜间 $(X/E)_t$ 的最大值^[33] 和平均值^[35] 计算 $(X/E)_0$. 本研究考虑到夜间最大值可能会受到异常

值影响, 而平均值则会导致计算的 $[\cdot\text{OH}] \times \Delta t$ 出现较多负值, 结合 $(X/E)_t$ 的平均日变化[图 2(a)], 最终选取夜间 $(X/E)_t$ 的第 85% 百分位数作为 $(X/E)_0$ (4.2). k_X 和 k_E 分别为间/对二甲苯和乙苯与 $\cdot\text{OH}$ 的反应速率常数, 数值为 $1.87 \times 10^{-11} \text{ cm}^3 \cdot (\text{molecule} \cdot \text{s})^{-1}$ 和 $7.0 \times 10^{-12} \text{ cm}^3 \cdot (\text{molecule} \cdot \text{s})^{-1}$ ^[34].

1.3 随机森林(RF)和SHAP算法

1.3.1 基于RF的O₃模拟及交叉验证

RF 是以决策树为基学习器构建的一种 Bagging 集成算法^[36]. 本研究使用 Python 中机器学习工具箱 scikit-learn 库中的 RandomForestRegressor 函数来建立近地面 O₃ 浓度与可解释变量之间的关系. 选取的可解释变量包括: 化学要素 (VOCs、NO_x、CO) 和气象要素 (WS、WD、RH、T). 构建 RF 时的关键参数包括决策树的数量 (n_estimators)、决策树的最大深度 (max_depth) 和节点可分的最小样本数 (min_samples_split). 本研究通过网格搜索的方法^[37,38] 调整这些参数使 O₃ 模拟值和实测值的 R² 最高, 最终确定了 n_estimators、max_depth 和 min_samples_split 的取值分别是 310、16 和 5, 其它 RF 参数设置为默认值. 在进行交叉验证时, 将归一化处理后的观测数据分为 10 个子集, 轮流交替选取其中一个子集作为测试数据, 其余 9 个子集作为训练数据. 利用决定系数 (R²)、平均绝对误差 (MAE)、平方根误差 (RMSE) 来

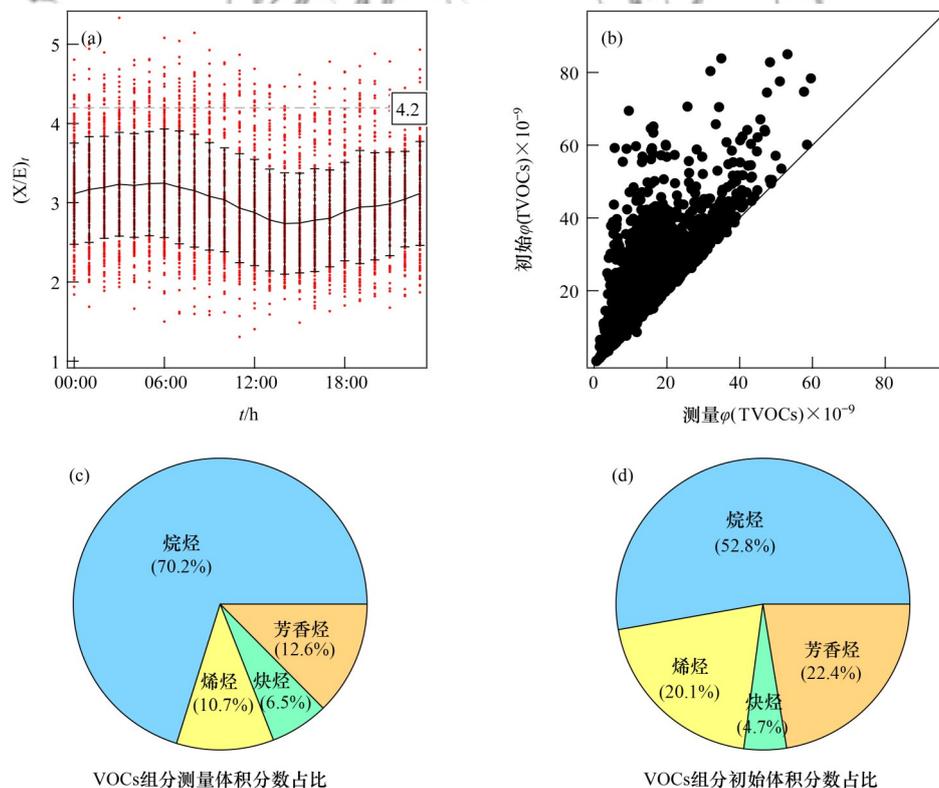


图 2 观测期间 $(X/E)_t$ 平均日变化、初始和测量 TVOCs 散点图、测量和初始 VOCs 化学组成

Fig. 2 Diurnal variation pattern of $(X/E)_t$, scatter plot of initial and measured TVOCs, chemical compositions of measured, and initial VOCs during the entire observation period

评估模型性能。

设置了3种方案对O₃浓度进行模拟(表1中方案A~C)。3种方案选取的可解释变量中NO_x、CO和气象要素保持一致,差别在于VOCs。方案A中选取了所有观测VOCs组分总的体积分数(TVOCs)作为一个特征变量,而方案B和C中则分别选择各VOCs组分的测量体积分数和初始体积分数作为特征变量。模拟时间均为2020年4~9月。

1.3.2 基于SHAP算法的特征变量贡献

SHAP是一种用于解释ML模型模拟结果的方法。基于合作博弈论中的Shapley值,为每个特征变量分配一个重要性值,以解释各个特征变量的贡献^[39]。本研究使用python中shap库对表1方案A、B和C中每个特征变量的贡献进行解释和量化。通过创建shap.Explainer对象来构建SHAP解释器,将RF模型和模型的训练数据传递给解释器。最后,使用解释器中的shap_values计算每个特征变量的SHAP值,公式如下:

$$O_{3(i)} = O_{3(\text{base})} + \sum_{j=1}^s \text{shap}(x_{ij}) \quad (3)$$

式中, O_{3(i)}为RF模型模拟的O₃浓度(样本*i*), O_{3(base)}为

O₃模拟浓度的平均值, shap(*x_{ij}*)为特征变量*j*对O_{3(i)}的贡献值。当shap(*x_{ij}*) > 0时,表示特征变量*j*对O_{3(i)}呈正贡献; shap(*x_{ij}*) < 0时,则特征变量*j*对O_{3(i)}呈负贡献。SHAP值计算方法的详细介绍参见文献[40]。

1.3.3 基于RF模型的多情景模拟

选取2020年4~9月VOCs数据完善的O₃污染天[即O₃日最大8h滑动浓度平均值ρ(DMA-8h O₃)大于160 μg·m⁻³或O₃日最大小时浓度平均值ρ(DMA-1h O₃)大于200 μg·m⁻³], 07:00~19:00作为O₃-VOCs-NO_x敏感性分析时段(表1方案D)。本研究考虑到VOCs初始体积分数校正了光化学消耗,在最近的研究中采用了VOCs初始体积分数作为RF模型的特征变量进行O₃-VOCs-NO_x敏感性分析^[29],因此,将VOCs初始体积分数作为方案D的特征变量之一。方案D作为RF的训练集(即基准情景),将特征变量NO_x浓度和VOCs初始体积分数分别从基准情景平均值的0.5倍以0.05倍间隔上升至1.5倍,模拟不同21×21个情景下DMA-8h O₃,并将其作为RF测试数据。通过多情景分析建立DMA-8h O₃与NO_x和VOCs的等值线(即EKMA曲线),进而判断O₃-VOCs-NO_x敏感性。

表1 基于RF的O₃模拟方案

Table 1 O₃ simulation scheme based on RF

方案编号	特征变量		模拟变量和时段
	气象要素	化学要素	
A		TVOCs、NO _x 和CO	O ₃ 小时值; 2020年4~9月
B	WS、WD、RH和T	测量VOCs、NO _x 和CO	
C		初始VOCs、NO _x 和CO	
D	同上	初始VOCs、NO _x 和CO	

1.4 基于观测的盒子模型(OBM)

本研究所使用的OBM在Cardelino和Chameides开发的0维盒子模型^[41]基础上将化学机制由CB04升级至CB05^[7],以O₃及其前体物和气象条件的观测数据逐时浓度作为约束,模拟近地面O₃生成过程,并计算O₃生成速率^[41]。OBM模拟时段与RF方案D保持一致,即O₃污染天的07:00~19:00。以VOCs、O₃、一氧化氮(NO)和CO,以及T的小时均值作为约束。通过与RF方案D中类似的多情景分析来得到EKMA曲线:以VOCs和NO_x观测数据的平均值作为基础情景,然后将其从0.5以0.05倍为间隔增至1.5倍,模拟21×21个情景下DMA-8h O₃,得到EKMA曲线。

2 结果与讨论

2.1 O₃及其前体物污染特征

2.1.1 O₃及其前体物浓度水平及时间变化

图3展示了2020年4~9月O₃及其前体物浓度和气象要素的时间变化。在观测期间,ρ(O₃)的平均值

为(86.1 ± 53.8) μg·m⁻³。ρ(DMA-8h O₃)在44.3~281.0 μg·m⁻³之间,平均值为(132.8 ± 45.9) μg·m⁻³,其中有56 d超过160 μg·m⁻³。ρ(DMA-1h O₃)在48.0~314.0 μg·m⁻³之间,平均值为(150.5 ± 51.0) μg·m⁻³,其中有30 d超过200 μg·m⁻³。O₃污染天和非污染天T、ρ(NO_x)、测量φ(TVOCs)的平均值分别为(26.2 ± 5.3) °C和(21.7 ± 6.1) °C、(34.3 ± 24.4) μg·m⁻³和(32.0 ± 25.2) μg·m⁻³、(15.4 ± 7.7) × 10⁻⁹和(13.3 ± 8.0) × 10⁻⁹,前者显著高于后者(2个独立样本*t*检验, *P* < 0.05)。

观测期间,初始φ(TVOCs)和测量φ(TVOCs)的平均值分别为(19.4 ± 12.7) × 10⁻⁹和(13.4 ± 7.9) × 10⁻⁹,前者显著高于后者(2个相关样本*t*检验, *P* < 0.05)。从二者的相关性分析也可以看出,初始与测量φ(VOCs)的比值均大于1[图2(b)]。从化学组成来看,测量φ(TVOCs)中的烷烃占比最高(70.2%),其次是芳香烃(12.6%)、烯烃(10.7%)和炔烃(6.5%)[图2(c)]。初始φ(VOCs)中,烯烃和芳香烃

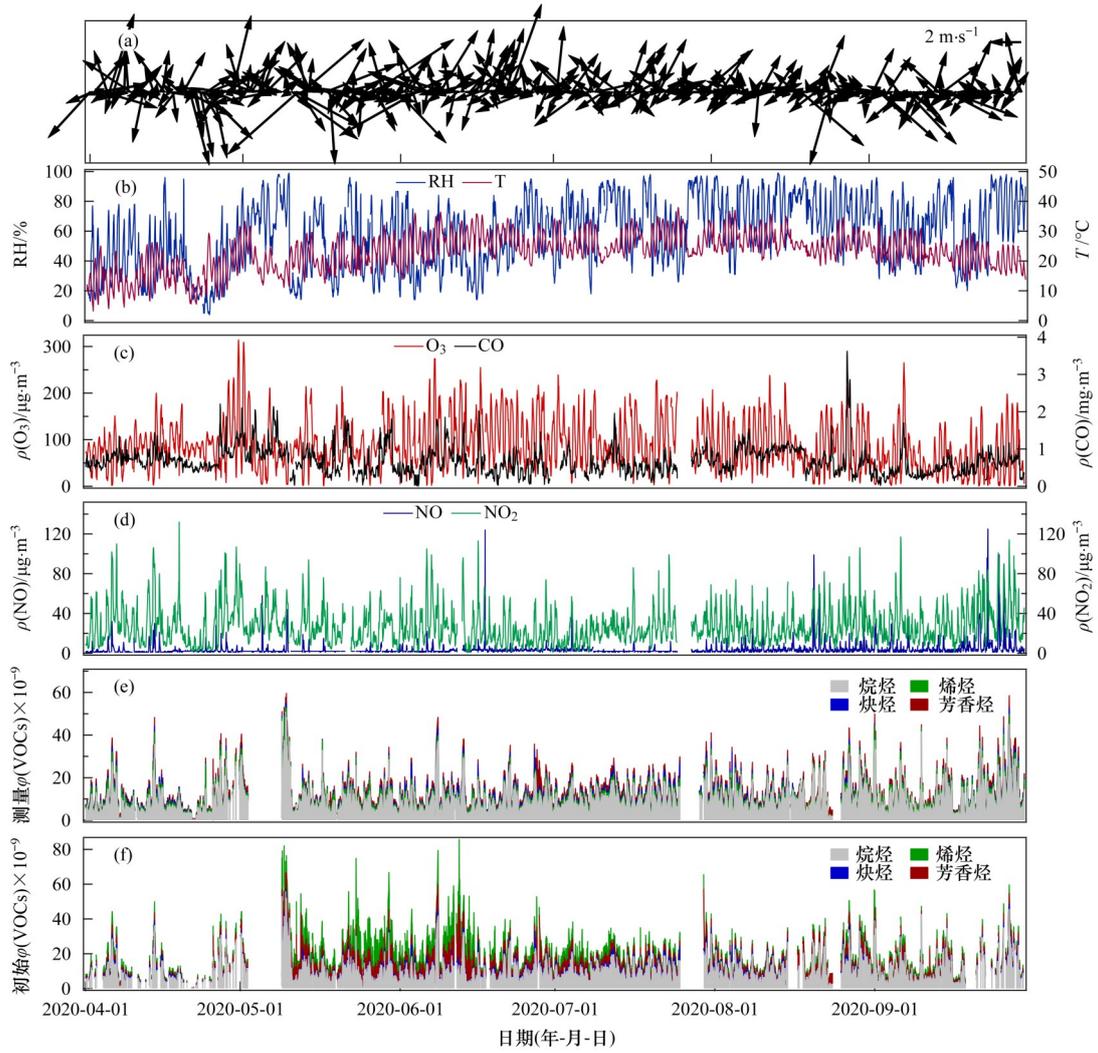


图3 观测期间WD、WS、T、RH、O₃、CO、NO、NO₂、测量VOCs和初始VOCs时间序列
 Fig. 3 Time series of WD, WS, T, RH, O₃, CO, NO, NO₂, measured VOCs, and initial VOCs

的体积分数占比分别增加至 20.1% 和 22.4%，而烷烃和炔烃体积分数占比则降低至 52.8% 和 4.7% [图 2(d)]。这表明光化学反应对活性强的烯烃和芳香烃体积分数有显著影响，不考虑 VOCs 光化学消耗，可能会低估高活性烯烃和芳香烃组分对 O₃ 生成的

影响。

2.1.2 O₃与化学要素和气象要素的相关性分析

图 4(a) 展示了观测期间 O₃ 小时均值与 NO_x、TVOCs、CO、T、RH 和 WS 小时值的相关性。结果显示：O₃ 与 T 呈显著正相关，其 Pearson 相关系数 r 为

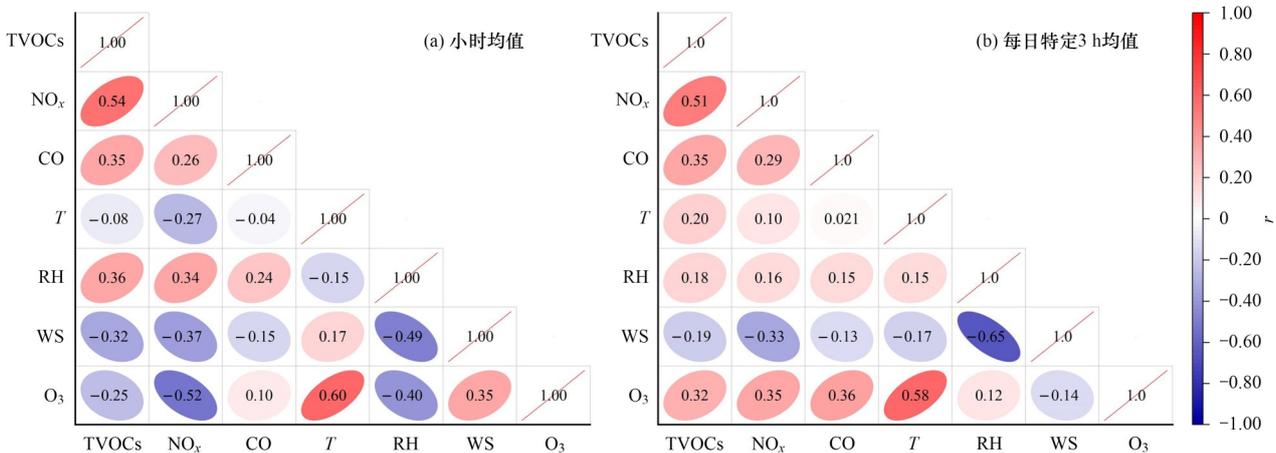


图4 观测期间 O₃ 与 NO_x、TVOCs、CO、T、RH 和 WS 的 Pearson 相关性分析

Fig. 4 Pearson correlation analyses of O₃ and NO_x, TVOCs, CO, T, RH, and WS during the entire observation period

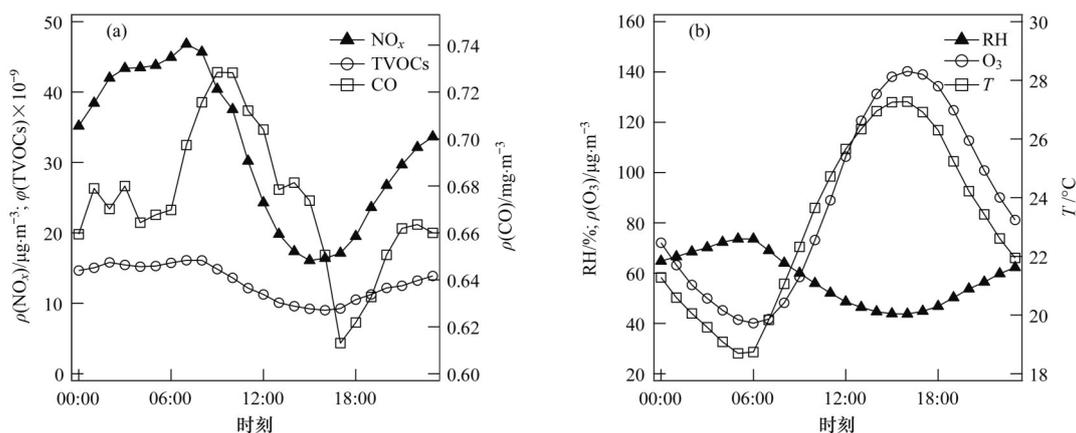


图5 观测期间 NO_x 、TVOCs、CO、RH、 O_3 和 T 的平均日变化特征

Fig. 5 Average diurnal variation patterns of NO_x , TVOCs, CO, RH, O_3 , and T during the entire observation period

0.60 ($P < 0.01$), 与 RH 呈显著负相关, r 为 -0.40 ($P < 0.01$), 表明高浓度的 O_3 通常伴随着高温低湿的气象条件^[42,43]. O_3 小时均值与 NO_x 和 TVOCs 呈显著负相关, r 分别为 -0.52 和 -0.25 ($P < 0.01$). 这是因为 O_3 生成伴随着 TVOCs 和 NO_x 的光化学消耗, 因此高浓度的 O_3 通常出现在午后, 而 NO_x 和 TVOCs 则在晚上和清晨出现高值(图 5).

为了评估逐日的 O_3 生成与化学要素和气象要素的关系, 本研究根据其平均日变化规律(图 5), 选取了 15:00 ~ 17:00 的 O_3 和 T 的平均值, 07:00 ~ 09:00 的 NO_x 、TVOCs、CO 和 RH 平均值进行 Pearson 相关性分析[图 4(b)]. O_3 与 T 呈显著正相关($r = 0.58$, $P < 0.01$), 与 TVOCs、 NO_x 和 CO 也呈正相关(r 为 0.32 ~ 0.36, $P < 0.01$). 这表明清晨高浓度 TVOCs、

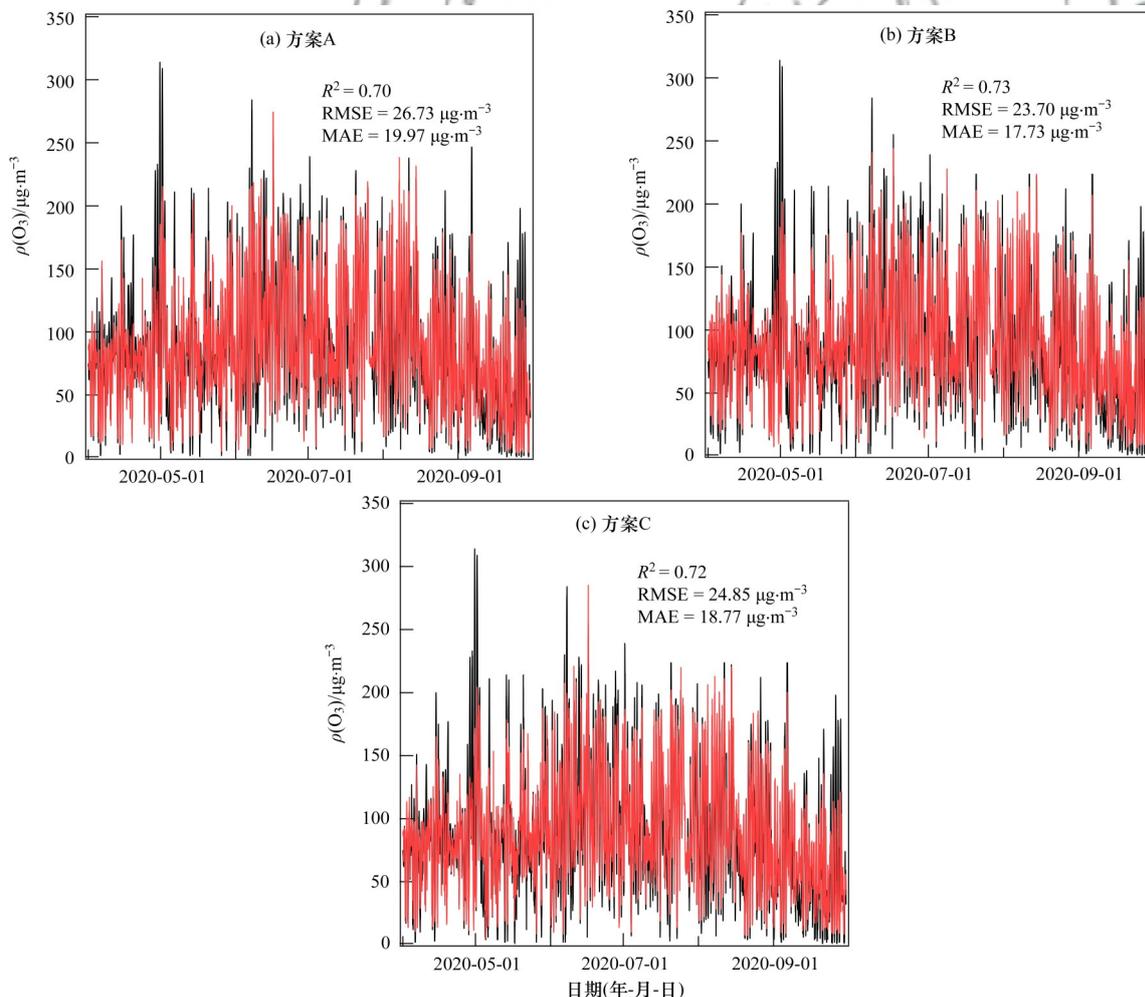


图6 RF 模拟的 O_3 与实测值的比较

Fig. 6 Comparisons of simulated and measured O_3 values for RF

NO_x和CO对当天O₃生成具有促进作用。

2.2 基于RF的O₃影响因素分析

2.2.1 RF模拟交叉验证

图6展示了利用RF按照表1中A~C这三种方案模拟的O₃与实测值之间的比较。红色和黑色的实线分别为O₃模拟值和O₃实测值的时间序列，结果显示，该模型模拟的O₃与实测值的变化趋势具有一致性，R²、RMSE和MAE分别为0.70~0.73、23.70~26.73 μg·m⁻³和17.73~19.97 μg·m⁻³。利用RF模拟O₃的研究显示R²、RMSE和MAE分别为0.57~0.87、10.13~31.45 μg·m⁻³和14.49~28.45 μg·m⁻³[24,44~48]，与以往研究所给出的性能评估指标相比，本研究中的R²和RMSE处于中等，表明RF对O₃的模拟结果可接受。

2.2.2 特征变量对O₃浓度的贡献

为评估各个特征变量对O₃模拟值的贡献，计算了方案A~C的SHAP值(图7)。图7(a)~7(c)中每个点代表一个样本，颜色代表特征变量的数值(即特

征值)的大小。从图7(d)~7(f)中可以看出，在方案A~C中，对O₃模拟值贡献(平均|SHAP值|)排在前4的特征变量分别是T、NO_x、CO和RH，但是不同特征变量的SHAP值正负存在差异。T和CO随着数值增加，相应的SHAP值增加，说明其对O₃模拟值是正向影响。NO_x和RH对O₃模拟值有负向影响，且随着NO_x和RH数值的增加负向影响越显著。

在方案A中，TVOCs对O₃模拟值贡献较低。在方案B和C中因为采用VOCs组分数据，因此可以分析不同组分对O₃模拟值的贡献。方案B和C，对O₃模拟值贡献较高的VOC组分相似，排名靠前的是苯、苯乙烯、乙烷、乙炔和正丁烷等。需要注意的是，方案B和C所计算得到的一些VOCs组分的平均|SHAP值|[图7(e)~7(f)]甚至高于方案A中TVOCs的平均|SHAP值|[图7(d)]，说明基于TVOCs来表征其对O₃模拟的影响时可能会存在一定程度的低估，这可能是将TVOCs作为一个特征变量来模拟O₃可能会掩盖一些组分的信息。

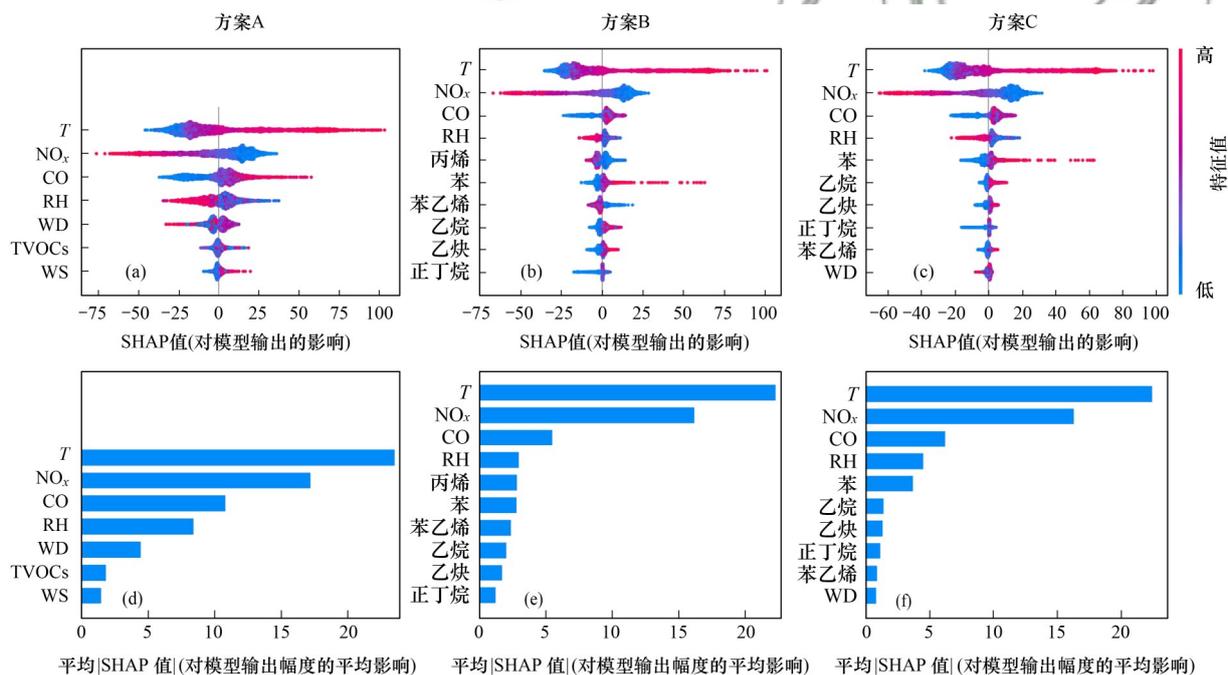


图7 各个特征变量的SHAP值

Fig. 7 SHAP values of each characteristic variable

2.3 O₃-VOCs-NO_x敏感性分析

在比较OBM与RF所给出的O₃-VOCs-NO_x敏感性之前，评估了OBM和RF对污染天O₃浓度的模拟效果。OBM模拟的O₃浓度与实测值吻合较好，R²、一致性指数(IOA)^[49]和RMSE分别为0.71、0.79和30.82 μg·m⁻³。以VOCs初始体积分数作为RF特征变量模拟的污染天O₃浓度与实测值的R²、RMSE和MAE分别为0.76、25.69 μg·m⁻³和19.80 μg·m⁻³，表

明RF能较好地模拟污染天的O₃浓度。进一步对两种方法模拟的DMA-8h O₃浓度进行比较。图8展示了RF模型和OBM模拟的多情景下DMA-8h O₃浓度相对误差，具体的情景设置参见1.3.3节。从图8中可以看出，两个模型给出的DMA-8h O₃浓度较为接近，其相对误差[(RF-OBM)/OBM]范围为0.07%~35.40%，平均值为11.71%。另外，越接近基准情景，RF模型和OBM模拟的DMA-8h O₃浓度相对误差越

低. 例如在 0.8 ~ 1.2 倍基准情景下(图 8 中黑色框), DMA-8h O_3 浓度相对误差的范围为 0.07% ~ 16.72%, 平均值为 5.81%, 显著低于 0.5 ~ 1.5 倍基准情景下的平均相对误差.

图 9 比较了利用 RF 模型和 OBM 得到的 O_3 污染天 O_3 生成的 EKMA 曲线, 其中黑点表示模拟时段内 VOCs 体积分数和 NO_x 浓度平均值, 即基准情景. RF 结果显示, 仅减少 VOCs 体积分数时, DMA-8h O_3 浓度随之下降, 仅减少 NO_x 浓度时, DMA-8h O_3 浓度不降反而上升, 表明 O_3 生成处于 VOCs 控制区[图 9 (a)]. 图 9(b) 中减少 NO_x 浓度或 VOCs 体积分数时 DMA-8h O_3 浓度的变化情况与 RF 模型的结果基本一致, 结果也表明 O_3 生成处于 VOCs 控制区. 说明 RF 模型进行 O_3 -VOCs- NO_x 敏感性分析具有良好的效果. 尽管 RF 模型等机器学习方法不考虑化学过程, 但本研究发现通过与 OBM 的比较其也能取得较好的效果, 而且其计算速度快, 是 O_3 -VOCs- NO_x 敏感性分析的一种重要的补充方法.

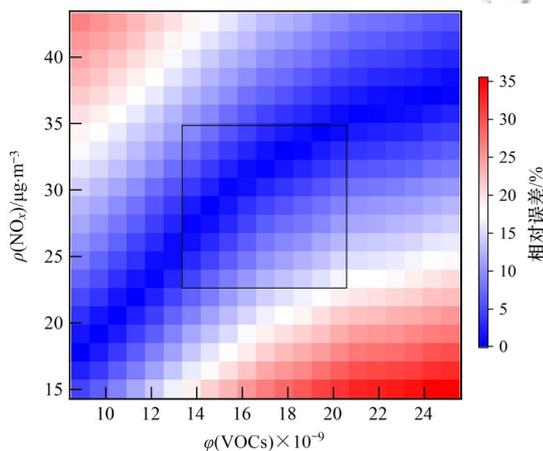
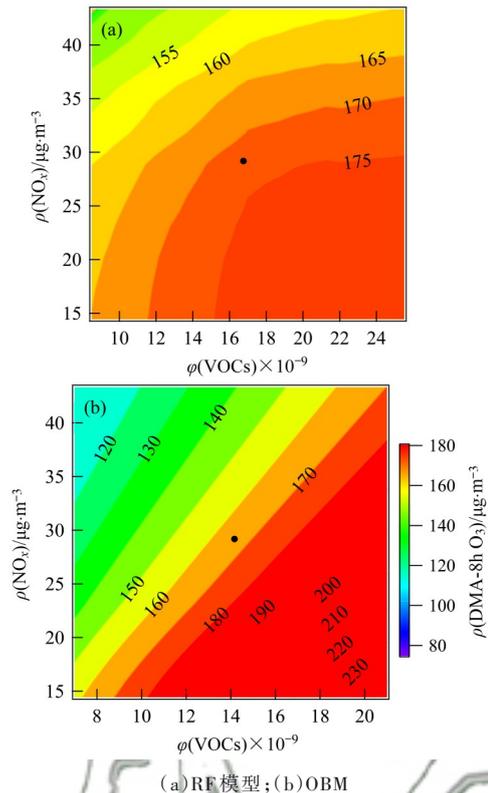


图 8 RF 模型和 OBM 模拟 DMA-8h O_3 浓度相对误差
Fig. 8 Relative errors of simulated DMA-8h O_3 concentration between the RF model and OBM

3 结论

(1) 2020 年 4 ~ 9 月在北京城区点的观测结果显示: ρ (DMA-8h O_3) 平均值为 $(132.8 \pm 45.9) \mu\text{g}\cdot\text{m}^{-3}$, 有 56 d 超过 $160 \mu\text{g}\cdot\text{m}^{-3}$; O_3 污染天 ρ (NO_x) 和 ϕ (TVOCs) 的平均值分别为 $(34.3 \pm 24.4) \mu\text{g}\cdot\text{m}^{-3}$ 和 $(15.4 \pm 7.7) \times 10^{-9}$, 显著高于非污染天. 从小时浓度来看, O_3 与 T 和 CO 呈显著正相关, 与 NO_x 和 TVOCs 呈现显著负相关. 而从每日特定 3 h 平均值来看, O_3 与 T 、TVOCs 和 NO_x 均呈显著正相关.

(2) 设置了 3 种方案利用 RF 模型模拟 O_3 , 模拟值与实测值吻合较好, R^2 、RMSE 和 MAE 分别为 0.70 ~ 0.73、23.70 ~ 26.73 $\mu\text{g}\cdot\text{m}^{-3}$ 和 17.73 ~ 19.97



(a) RF 模型; (b) OBM
图 9 O_3 污染天 DMA-8h O_3 浓度的 EKMA 曲线
Fig. 9 EKMA curves of DMA-8h O_3 concentration during O_3 pollution days

$\mu\text{g}\cdot\text{m}^{-3}$. SHAP 值计算结果显示 NO_x 和 RH 对 O_3 有负向影响, 而 VOCs 和 CO 有正向影响. 对 O_3 模拟值贡献较高的 VOC 组分是苯、苯乙烯、乙烷、乙炔和正丁烷等.

(3) 选择 O_3 污染天 VOCs 和 NO_x 平均值作为基准情景, 以 0.05 倍为间隔设置 0.5 倍至 1.5 倍的 21×21 个情景. 利用 RF 模型模拟不同情景下 DMA-8h O_3 浓度进而得到 EKMA 曲线, 结果表明 O_3 生成处于 VOCs 控制区, 与 OBM 结果相一致. 这说明 RF 模型可以作为化学传输模型的重要补充方法用于 O_3 -VOCs- NO_x 敏感性分析.

致谢: 本研究的数值计算得到了南京信息工程大学高性能计算中心的支持和帮助.

参考文献:

- [1] Niu Z P, Duan Z Z, Wei J, *et al.* Associations of long-term exposure to ambient ozone with hypertension, blood pressure, and the mediation effects of body mass index: a national cross-sectional study of middle-aged and older adults in China [J]. *Ecotoxicology and Environmental Safety*, 2022, **242**, doi: 10.1016/J.ECOENV.2022.113901.
- [2] Ou J M, Huang Z J, Klimont Z, *et al.* Role of export industries on ozone pollution and its precursors in China [J]. *Nature Communications*, 2020, **11** (1), doi: 10.1038/s41467-020-19035-x.
- [3] Li H M, Yang Y, Jin J B, *et al.* Climate-driven deterioration of future ozone pollution in Asia predicted by machine learning with multi-source data [J]. *Atmospheric Chemistry and Physics*, 2023,

- 23(2): 1131-1145.
- [4] Ainsworth E A, Yendrek C R, Stith S, *et al.* The effects of tropospheric ozone on net primary productivity and implications for climate change [J]. *Annual Review of Plant Biology*, 2012, **63**: 637-661.
- [5] 中华人民共和国生态环境部. 2020年中国生态环境状况公报 [EB/OL]. <https://www.mee.gov.cn/hjzl/sthjzk/zghjzkgb/202105/P020210526572756184785.pdf>, 2023-01-01.
- [6] Wang M, Chen W T, Zhang L, *et al.* Ozone pollution characteristics and sensitivity analysis using an observation-based model in Nanjing, Yangtze River Delta Region of China [J]. *Journal of Environmental Sciences*, 2020, **93**: 13-22.
- [7] Xu D N, Yuan Z B, Wang M, *et al.* Multi-factor reconciliation of discrepancies in ozone-precursor sensitivity retrieved from observation- and emission-based models [J]. *Environment International*, 2022, **158**, doi: 10.1016/J.ENVINT.2021.106952.
- [8] Tan Z F, Lu K D, Dong H B, *et al.* Explicit diagnosis of the local ozone production rate and the ozone-NO_x-VOC sensitivities [J]. *Science Bulletin*, 2018, **63**(16): 1067-1076.
- [9] Guo H, Chen K Y, Wang P F, *et al.* Simulation of summer ozone and its sensitivity to emission changes in China [J]. *Atmospheric Pollution Research*, 2019, **10**(5): 1543-1552.
- [10] Luo H H, Zhao K H, Yuan Z B, *et al.* Emission source-based ozone isopleth and isosurface diagrams and their significance in ozone pollution control strategies [J]. *Journal of Environmental Sciences*, 2021, **105**: 138-149.
- [11] 陆晓波, 王鸣, 丁峰, 等. 2020年和2021年南京城区臭氧生成敏感性和VOCs来源变化分析[J]. *环境科学*, 2023, **44**(4): 1943-1953.
- Lu X B, Wang M, Ding F, *et al.* Changes in O₃-VOCs-NO_x sensitivity and VOCs sources at an urban site of Nanjing between 2020 and 2021 [J]. *Environmental Science*, 2023, **44**(4): 1943-1953.
- [12] 钱骏, 徐晨曦, 陈军辉, 等. 2020年成都市典型臭氧污染过程特征及敏感性[J]. *环境科学*, 2021, **42**(12): 5736-5746.
- Qian J, Xu C X, Chen J H, *et al.* Chemical characteristics and contaminant sensitivity during the typical ozone pollution processes of Chengdu in 2020 [J]. *Environmental Science*, 2021, **42**(12): 5736-5746.
- [13] 孙晓艳, 赵敏, 申恒青, 等. 济南市城区夏季臭氧污染过程及来源分析[J]. *环境科学*, 2022, **43**(2): 686-695.
- Sun X Y, Zhao M, Shen H Q, *et al.* Ozone formation and key VOCs of a continuous summertime O₃ pollution event in Ji'nan [J]. *Environmental Science*, 2022, **43**(2): 686-695.
- [14] Wang L, Zhao Y, Shi J S, *et al.* Predicting ozone formation in petrochemical industrialized Lanzhou city by interpretable ensemble machine learning [J]. *Environmental Pollution*, 2023, **318**, doi: 10.1016/J.ENVPOL.2022.120798.
- [15] Cheng Y, Huang X F, Peng Y, *et al.* A novel machine learning method for evaluating the impact of emission sources on ozone formation [J]. *Environmental Pollution*, 2023, **316**, doi: 10.1016/J.ENVPOL.2022.120685.
- [16] Beddows A V, Kitwiroon N, Williams M L, *et al.* Emulation and sensitivity analysis of the community multiscale air quality model for a UK ozone pollution episode [J]. *Environmental Science & Technology*, 2017, **51**(11): 6229-6236.
- [17] Wang M, Shao M, Chen W, *et al.* A temporally and spatially resolved validation of emission inventories by measurements of ambient volatile organic compounds in Beijing, China [J]. *Atmospheric Chemistry and Physics*, 2014, **14**(12): 5871-5891.
- [18] Tang X, Zhu J, Wang Z F, *et al.* Improvement of ozone forecast over Beijing based on ensemble Kalman filter with simultaneous adjustment of initial conditions and emissions [J]. *Atmospheric Chemistry and Physics*, 2011, **11**(24): 12901-12916.
- [19] 侯墨, 蒋小梅, 赵文鹏, 等. 2021年夏季新乡市城区臭氧超标日污染特征及敏感性[J]. *环境科学*, 2023, **44**(5): 2472-2480.
- Hou M, Jiang X M, Zhao W P, *et al.* Ozone pollution characteristics and sensitivity during the ozone pollution days in summer 2021 of Xinxiang City [J]. *Environmental Science*, 2023, **44**(5): 2472-2480.
- [20] 伏志强, 戴春皓, 王章玮, 等. 长沙市夏季大气臭氧生成对前体物的敏感性分析[J]. *环境化学*, 2019, **38**(3): 531-538.
- Fu Z Q, Dai C H, Wang Z W, *et al.* Sensitivity analysis of atmospheric ozone formation to its precursors in summer of Changsha [J]. *Environmental Chemistry*, 2019, **38**(3): 531-538.
- [21] Feng R, Zheng H J, Zhang A R, *et al.* Unveiling tropospheric ozone by the traditional atmospheric model and machine learning, and their comparison: a case study in Hangzhou, China [J]. *Environmental Pollution*, 2019, **252**: 366-378.
- [22] Zheng H, Kong S F, He Y *et al.* Enhanced ozone pollution in the summer of 2022 in China: the roles of meteorology and emission variations [J]. *Atmospheric Environment*, 2023, **301**, doi: 10.1016/J.ATMOSENV.2023.119701.
- [23] 蔡旺华. 运用机器学习方法预测空气中臭氧浓度[J]. *中国环境管理*, 2018, **10**(2): 78-84.
- Cai W H. Using machine learning method for predicting the concentration of ozone in the air [J]. *Chinese Journal of Environmental Management*, 2018, **10**(2): 78-84.
- [24] Zhan Y, Luo Y Z, Deng X F, *et al.* Spatiotemporal prediction of daily ambient ozone levels across China using random forest for human exposure assessment [J]. *Environmental Pollution*, 2018, **233**: 464-473.
- [25] Fan K, Dhammapala R, Harrington K, *et al.* Development of a machine learning approach for local-scale ozone forecasting: application to Kennewick, WA [J]. *Frontiers in Big Data*, 2022, **5**, doi: 10.3389/FDATA.2022.781309.
- [26] Han H, Liu J, Shu L, *et al.* Local and synoptic meteorological influences on daily variability in summertime surface ozone in Eastern China [J]. *Atmospheric Chemistry and Physics*, 2020, **20**(1): 203-222.
- [27] Eslami E, Choi Y, Lops Y, *et al.* A real-time hourly ozone prediction system using deep convolutional neural network [J]. *Neural Computing and Applications*, 2020, **32**(13): 8783-8797.
- [28] Kalbande R, Kumar B, Maji S, *et al.* Machine learning based quantification of VOC contribution in surface ozone prediction [J]. *Chemosphere*, 2023, **326**, doi: 10.1016/J.CHEMOSPHERE.2023.138474.
- [29] Zhan J L, Liu Y C, Ma W, *et al.* Ozone formation sensitivity study using machine learning coupled with the reactivity of volatile organic compound species [J]. *Atmospheric Measurement Techniques*, 2022, **15**(5): 1511-1520.
- [30] Wang M, Zeng L M, Lu S H, *et al.* Development and validation of a cryogen-free automatic gas chromatograph system (GC-MS/FID) for online measurements of volatile organic compounds [J]. *Analytical Methods*, 2014, **6**(23): 9424-9434.
- [31] 姚青, 韩素芹, 张裕芬, 等. 天津夏季郊区VOCs对臭氧生成的影响[J]. *环境科学*, 2020, **41**(4): 1573-1581.
- Yao Q, Han S Q, Zhang Y F, *et al.* Effects of VOCs on ozone formation in the Tianjin suburbs in summer [J]. *Environmental*

- Science, 2020, **41**(4): 1573-1581.
- [32] 王玥, 魏巍, 任云婷, 等. 基于卫星遥感和地面观测的人为源 VOCs 区域清单多维校验[J]. 环境科学, 2021, **42**(6): 2713-2720.
Wang Y, Wei W, Ren Y T, *et al.* Multidimensional verification of anthropogenic VOCs emissions inventory through satellite retrievals and ground observations [J]. Environmental Science, 2021, **42**(6): 2713-2720.
- [33] 胡君, 王淑兰, 吴亚君, 等. 北京怀柔 O₃ 污染过程初始 VOCs 浓度特征及来源分析[J]. 环境科学研究, 2019, **32**(5): 766-775.
Hu J, Wang S L, Wu Y J, *et al.* Characteristics and source analysis of initial mixing ratio of atmospheric VOCs during an ozone episode in Huairou, Beijing [J]. Research of Environmental Sciences, 2019, **32**(5): 766-775.
- [34] 吴方堃, 王跃思, 安俊琳, 等. 北京奥运时段 VOCs 浓度变化、臭氧产生潜势及来源分析研究[J]. 环境科学, 2010, **31**(1): 10-16.
Wu F K, Wang Y S, An J L, *et al.* Study on concentration, ozone production potential and sources of VOCs in the atmosphere of Beijing during Olympics period [J]. Environmental Science, 2010, **31**(1): 10-16.
- [35] 罗瑞雪, 刘保双, 梁丹妮, 等. 天津市郊夏季的臭氧变化特征及其前体物 VOCs 的来源解析[J]. 环境科学, 2021, **42**(1): 75-87.
Luo R X, Liu B S, Liang D N, *et al.* Characteristics of ozone and source apportionment of the precursor VOCs in Tianjin suburbs in summer [J]. Environmental Science, 2021, **42**(1): 75-87.
- [36] Breiman L. Random forests [J]. Machine Learning, 2001, **45**(1): 5-32.
- [37] Ma R M, Ban J, Wang Q, *et al.* Random forest model based fine scale spatiotemporal O₃ trends in the Beijing-Tianjin-Hebei region in China, 2010 to 2017 [J]. Environmental Pollution, 2021, **276**, doi: 10.1016/j.envpol.2021.116635.
- [38] 姚红岩, 施润和. 基于周边站点优化选取的随机森林 PM_{2.5} 小时浓度预测研究[J]. 环境科学学报, 2021, **41**(4): 1565-1573.
Yao H Y, Shi R H. Research on hourly PM_{2.5} concentration prediction of random forest based on optimal selection of surrounding stations [J]. Acta Scientiae Circumstantiae, 2021, **41**(4): 1565-1573.
- [39] Ghahremanloo M, Choi Y, Lops Y. Deep learning mapping of surface MDA8 ozone: the impact of predictor variables on ozone levels over the contiguous United States [J]. Environmental Pollution, 2023, **326**, doi: 10.1016/j.envpol.2023.121508.
- [40] 董佳奇, 胡冬梅, 闫雨龙, 等. 基于可解释性机器学习的城市 O₃ 驱动因素挖掘[J]. 环境科学, 2023, **44**(7): 3660-3668.
Dong J Q, Hu D M, Yan Y L, *et al.* Revealing driving factors of urban O₃ based on explainable machine learning [J]. Environmental Science, 2023, **44**(7): 3660-3668.
- [41] Cardelino C A, Chameides W L. An observation-based model for analyzing ozone precursor relationships in the urban atmosphere [J]. Journal of the Air & Waste Management Association, 1995, **45**(3): 161-180.
- [42] 王雨燕, 杨文, 王秀艳, 等. 淄博市城郊臭氧污染特征及影响因素分析[J]. 环境科学, 2022, **43**(1): 170-179.
Wang Y Y, Yang W, Wang X Y, *et al.* Characteristics of ozone pollution and influencing factors in urban and suburban areas in Zibo [J]. Environmental Science, 2022, **43**(1): 170-179.
- [43] 刘建, 吴兑, 范绍佳, 等. 前体物与气象因子对珠江三角洲臭氧污染的影响[J]. 中国环境科学, 2017, **37**(3): 813-820.
Liu J, Wu D, Fan S J, *et al.* Impacts of precursors and meteorological factors on ozone pollution in Pearl River Delta [J]. China Environmental Science, 2017, **37**(3): 813-820.
- [44] 刘玉, 蔡秋亮, 佟磊, 等. 海陆风对宁波东南滨海郊区大气臭氧变化特征及预测的影响[J]. 环境科学学报, 2023, **43**(4): 27-39.
Liu Y, Cai Q L, Tong L, *et al.* Influence of sea-land breeze on the variation characteristics and prediction of ozone in the suburban coastal atmosphere of southeast Ningbo [J]. Acta Scientiae Circumstantiae, 2023, **43**(4): 27-39.
- [45] 何琰, 林惠娟, 曹舒娅, 等. 城市臭氧污染特征与高影响气象因子: 以苏州为例[J]. 环境科学, 2023, **44**(1): 85-93.
He Y, Lin H J, Cao S Y, *et al.* Characteristics of ozone pollution and high-impact meteorological factors in urban cities: a case of Suzhou [J]. Environmental Science, 2023, **44**(1): 85-93.
- [46] 赵楠, 卢毅敏. 中国地表臭氧浓度估算及健康影响评估[J]. 环境科学, 2022, **43**(3): 1235-1245.
Zhao N, Lu Y M. Estimation of surface ozone concentration and health impact assessment in China [J]. Environmental Science, 2022, **43**(3): 1235-1245.
- [47] Lyu Y, Ju Q R, Lv F M, *et al.* Spatiotemporal variations of air pollutants and ozone prediction using machine learning algorithms in the Beijing-Tianjin-Hebei region from 2014 to 2021 [J]. Environmental Pollution, 2022, **306**, doi: 10.1016/j.envpol.2022.119420.
- [48] 丁榛, 陈报章, 王瑾, 等. 基于决策树的统计预报模型在臭氧浓度时空分布预测中的应用研究[J]. 环境科学学报, 2018, **38**(8): 3229-3242.
Ding S, Chen B Z, Wang J, *et al.* An applied research of decision-tree based statistical model in forecasting the spatial-temporal distribution of O₃ [J]. Acta Scientiae Circumstantiae, 2018, **38**(8): 3229-3242.
- [49] He Z R, Wang X M, Ling Z H, *et al.* Contributions of different anthropogenic volatile organic compound sources to ozone formation at a receptor site in the Pearl River Delta region and its policy implications [J]. Atmospheric Chemistry and Physics, 2019, **19**(13): 8801-8816.

CONTENTS

Spatial Distribution Characteristics of PM _{2.5} and O ₃ in Beijing-Tianjin-Hebei Region Based on Time Series Decomposition	YAO Qing, DING Jing, YANG Xu, <i>et al.</i> (2487)
Ozone Sensitivity Analysis in Urban Beijing Based on Random Forest	ZHOU Hong, WANG Ming, CHAI Wen-xuan, <i>et al.</i> (2497)
Prediction of Ozone Pollution in Sichuan Basin Based on Random Forest Model	YANG Xiao-tong, KANG Ping, WANG An-yi, <i>et al.</i> (2507)
Establishment and Effective Evaluation of Haikou Ozone Concentration Statistical Prediction Model	FU Chuan-bo, LIN Jian-xing, TANG Jia-xiang, <i>et al.</i> (2516)
Spatial and Temporal Distribution Characteristics of Ozone Concentration and Health Benefit Assessment in the Beijing-Tianjin-Hebei Region from 2015 to 2020	GAO Ran, LI Qin, CHE Fei, <i>et al.</i> (2525)
Water-soluble Inorganic Ion Content of PM _{2.5} and Its Change Characteristics in Urban Area of Beijing in 2022	CHEN Yuan-yuan, CUI Di, ZHAO Ze-xi, <i>et al.</i> (2537)
Pollution Characteristics, Source, and Health Risk Assessment of Metal Elements in PM _{2.5} Between Winter and Spring in Zhengzhou	TAO Jie, YAN Hui-jiao, XU Yi-fei, <i>et al.</i> (2548)
Characteristics, Sources Apportionment, and Health Risks of PM _{2.5} -bound PAHs and Their Derivatives Before and After Heating in Zibo City	SUN Gang-li, WU Li-ping, XU Bo, <i>et al.</i> (2558)
Components Characteristic and Source Apportionment of Fine Particulate Matter in Transition Period of Heating Season in Xi'an with High Time Resolution	LI Meng-jin, ZHANG Yong, ZHANG Qian, <i>et al.</i> (2571)
Source and Cause Analysis of High Concentration of Inorganic Aerosol During Two Typical Pollution Processes in Winter over Tianjin	LU Miao-miao, HAN Su-qin, LIU Ke-xin, <i>et al.</i> (2581)
Spatial-temporal Variation and Spatial Differentiation Geographic Detection of PM _{2.5} Concentration in the Shandong Province Based on Spatial Scale Effect	XU Yong, WEI Meng-xin, ZOU Bin, <i>et al.</i> (2596)
Characteristics of VOCs Emissions and Ozone Formation Potential for Typical Chemicals Industry Sources in China	WU Ting, CUI Huan-wen, XIAO Xian-de, <i>et al.</i> (2613)
Formation Potential of Secondary Organic Aerosols and Sources of Volatile Organic Compounds During an Air Pollution Episode in Autumn, Langfang	ZHANG Jing-qiao, LIU Zheng, DING Wen-wen, <i>et al.</i> (2622)
Scale Effects of Landscape Pattern on Impacts of River Water Quality: A Meta-analysis	WANG Yu-cang, DU Jing-jing, ZHANG Yu, <i>et al.</i> (2631)
Spectral Characteristics and Sources of Dissolved Organic Matter in Inflow Rivers of Baiyangdian Lake Water in Summer Flood Season	MENG Jia-jing, DOU Hong, CHEN Zhe, <i>et al.</i> (2640)
Analysis on Hydrochemical Evolution of Shallow Groundwater East of Yongding River in Fengtai District, Beijing	HU Yu-xin, ZHOU Rui-jing, SONG Wei, <i>et al.</i> (2651)
Hydrochemical Characteristics, Controlling Factors and Water Quality Evaluation of Shallow Groundwater in Tan-Lu Fault Zone (Anhui Section)	LIU Hai, WEI Wei, SONG Yang, <i>et al.</i> (2665)
Effects of Pesticides Use on Pesticides Residues and Its Environmental Risk Assessment in Xingkai Lake (China)	WANG Wei-qing, XU Xiong, LIU Quan-zhen, <i>et al.</i> (2678)
Characteristics of Microorganisms and Antibiotic Resistance Genes of the Riparian Soil in the Lanzhou Section of the Yellow River	WEI Cheng-chen, WEI Feng-yi, XIA Hui, <i>et al.</i> (2686)
Analysis of the Spatiotemporal Distribution of Algal Blooms and Its Driving Factors in Chaohu Lake Based on Multi-source Datasets	JIN Xiao-long, DENG Xue-liang, DAI Rui, <i>et al.</i> (2694)
Characteristics of Epiphytic Bacterial Community on Submerged Macrophytes in Water Environment Supplemented with Reclaimed Water	HE Yun, LI Xue-mei, LI Hong-quan, <i>et al.</i> (2707)
Effects of Water Level Fluctuations and Vegetation Restoration on Soil Prokaryotic Microbial Community Structure in the Riparian Zone of the Three Gorges Reservoir	MEI Yu, HUANG Ping, WANG Peng, <i>et al.</i> (2715)
Bacterial Community Structure of Typical Lake Sediments in Yinchuan City and Its Response to Heavy Metals	MENG Jun-jie, LIU Shuang-yu, QIU Xiao-cong, <i>et al.</i> (2727)
Effect of Thermal Hydrolysis Pretreatment Time on Microbial Community Structure in Sludge Anaerobic Digestion System	ZHANG Han, ZHANG Han, WANG Jia-wei, <i>et al.</i> (2741)
Source Apportionment of Morphine in Wastewater	SHAO Xue-ting, ZHAO Yue-tong, JIANG Bing, <i>et al.</i> (2748)
Ecological Environment Dynamical Evaluation of Hutuo River Basin Using Remote Sensing	LI Yan-cui, YUAN Jin-guo, LIU Bo-han, <i>et al.</i> (2757)
Spatiotemporal Evolution and Influencing Factors of Ecosystem Service Value in the Yellow River Basin	WANG Yi-qi, SUN Xue-ying (2767)
Ecosystem Service Trade-off Synergy Strength and Spatial Pattern Optimization Based on Bayesian Network: A Case Study of the Fenhe River Basin	CAI Jin, WEI Xiao-jian, JIANG Ping, <i>et al.</i> (2780)
Spatial-temporal Evolution and Quantitative Attribution of Habitat Quality in Typical Karst Counties of Guizhou Plateau	LI Yue, FENG Xia, WU Lu-hua, <i>et al.</i> (2793)
Spatial-temporal Variation in NEP in Ecological Zoning on the Loess Plateau and Its Driving Factors from 2000 to 2021	ZHOU Yi-ting, YAN Jun-xia, LIU Ju, <i>et al.</i> (2806)
Land Change Simulation and Grassland Carbon Storage in the Loess Plateau Based on SSP-RCP Scenarios	CUI Xie, DONG Yan, ZHANG Lu-yin, <i>et al.</i> (2817)
Multi-scenario Simulation of Construction Land Expansion and Its Impact on Ecosystem Carbon Storage in Beijing-Tianjin-Hebei Urban Agglomeration	WU Ai-bin, CHEN Fu-guo, ZHAO Yan-xia, <i>et al.</i> (2828)
Effects of Land Use Change on Soil Aggregate Stability and Soil Aggregate Organic Carbon in Karst Area of Southwest China	JIANG Ke, JIA Ya-nan, YANG Yan, <i>et al.</i> (2840)
Integrated Analysis of Soil Organic Matter Molecular Composition Changes Under Different Land Uses	HUANG Shi-wei, ZHAO Yi-kai, ZHU Xin-yu, <i>et al.</i> (2848)
Prediction Spatial Distribution of Soil Organic Matter Based on Improved BP Neural Network with Optimized Sparrow Search Algorithm	HU Zhi-ru, ZHAO Wan-fu, SONG Yin-xian, <i>et al.</i> (2859)
Effects of Application of Different Organic Materials on Phosphorus Accumulation and Transformation in Vegetable Fields	SUN Kai, CUI Yu-tao, LI Shun-jin, <i>et al.</i> (2871)
Intensive Citrus Cultivation Suppresses Soil Phosphorus Cycling Microbial Activity	ZHOU Lian-hao, ZENG Quan-chao, MEI Tang-ying-ze, <i>et al.</i> (2881)
Effects of Controlled-release Blended Fertilizer on Crop Yield and Greenhouse Gas Emissions in Wheat-maize Rotation System	GAO Wei, WANG Xue-xia, XIE Jian-zhi, <i>et al.</i> (2891)
Effect of Biochar on NO ₃ ⁻ -N Transport in Loessial Soil and Its Simulation	BAI Yi-ru, LIU Xu, ZHANG Yu-han, <i>et al.</i> (2905)
Analysis and Evaluation of Heavy Metal Pollution in Farmland Soil in China: A Meta-analysis	YANG Li, BAI Zong-xu, BO Wen-hao, <i>et al.</i> (2913)
Critical Review on Heavy Metal Contamination in Urban Soil and Surface Dust	WANG Xiao-yu, LIU En-feng, YANG Xiang-meng, <i>et al.</i> (2926)
Research Progress on Solidification and MICP Remediation of Soils in Heavy Metal Contaminated Site	CHEN Yue-ru, GAO Wen-yan, CHEN Hong-ren, <i>et al.</i> (2939)
Pollution Characteristics and Source Analysis of Soil Heavy Metal in Coal Mine Area near the Yellow River in Shandong	DAI Wen-ting, ZHANG Hui, WU Xia, <i>et al.</i> (2952)
Heavy Metal Content and Risk Assessment of Sediments and Soils in the Juma River Basin	HAN Shuang-bao, YUAN Lei, ZHANG Qiu-xia, <i>et al.</i> (2962)
Characteristics, Ecological Risk Assessment, and Source Apportionment of Soil Heavy Metals in the Yellow River Floodplain of Yinchuan City	YU Lu-jia, MA Hai-jun, WANG Cui-ping (2971)
Health Risk Assessment of Heavy Metals in Soils of a City in Guangdong Province Based on Source Oriented and Monte Carlo Models	CHEN Lian, ZOU Zi-hang, ZHANG Pei-zhen, <i>et al.</i> (2983)
Chemical Speciation, Influencing Factors, and Regression Model of Heavy Metals in Farmland of Typical Carbonate Area with High Geological Background, Southwest China	TANG Rui-ling, XU Jin-li, LIU Bin, <i>et al.</i> (2995)
Hg Content Characteristics and Safe Planting Zoning of Paddy Soil and Rice in Guizhou Province	WEI Mei-liu, ZHOU Lang, HUANG Yan-ling, <i>et al.</i> (3005)
Cadmium Phytoremediation Effect of Sweet Sorghum Assisted with Citric Acid on Typical Parent Soil in Southern China	LIU Meng-yu, LUO Xu-feng, GU Jiao-feng, <i>et al.</i> (3016)
Effects of Modified Distillers' Grains Biochar on Cadmium Forms in Purple Soil and Cadmium Uptake by Rice	XIAO Nai-chuan, WANG Zi-fang, YANG Wen-na, <i>et al.</i> (3027)
Effects of Biochar on Growth and Pollutant Accumulation of Lettuce in Soil Co-contaminated with Tetracycline and Copper	ZHENG Chen-ge, PEI Huan-huan, ZHANG Ya-shan, <i>et al.</i> (3037)
Effects of Vermicomposting on Compost Quality and Heavy Metals: A Meta-analysis	JIANG Ji-shao, HOU Rui, CUI Hui-lin, <i>et al.</i> (3047)
Advances in the Effects of Microplastics on Soil N ₂ O Emissions and Nitrogen Transformation	LIU Yi-ge, YANG An-qi, CHEN Shu-xin, <i>et al.</i> (3059)
Effects of Land Use Patterns on Soil Microplastic Pollution in the Luoshijiang Sub-watershed of Erhai Lake Basin	DAI Liu-yun, HOU Lei, WANG Hua, <i>et al.</i> (3069)
Characteristics of Microplastic Pollution in Sediment of Silty Coast in Culture Bay	SONG Ke-xin, HE Jin-cheng, LI Chang-hua, <i>et al.</i> (3078)
Effect of Polyethylene Microplastics on the Microbial Community of Saline Soils	WANG Zhi-chao, LI Zhe, LI Jia-chen, <i>et al.</i> (3088)
Characterization of Microplastic Surface Bacterial Community Structure and Prediction of Ecological Risk in Poyang Lake, China	YU Jin-li, ZHAO Jun-kai, LUO Si-qi, <i>et al.</i> (3098)
Energy-saving and Emission Reduction Path for Road Traffic in Key Coastal Cities of Guangdong, Fujian and Zhejiang	XU Yi-nuo, WENG Da-wei, WANG Shuo, <i>et al.</i> (3107)
Life Cycle Carbon Reduction Benefits of Electric Heavy-duty Truck to Replace Diesel Heavy-duty Truck	XU Yuan-yuan, GONG De-hong, HUANG Zheng-guang, <i>et al.</i> (3119)